Nanoscale

Accepted Manuscript

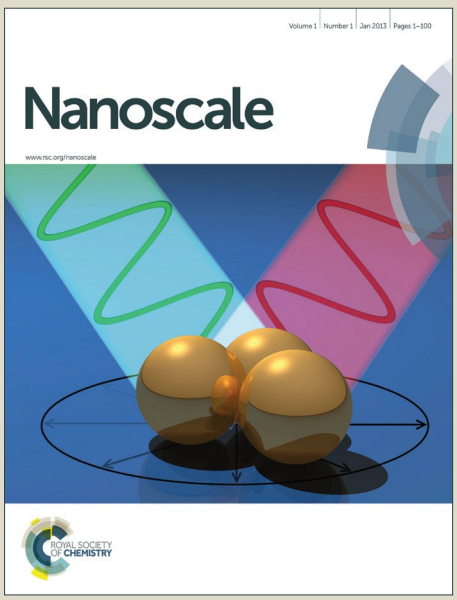

This is an *Accepted Manuscript*, which has been through the Royal Society of Chemistry peer review process and has been accepted for publication.

Accepted Manuscripts are published online shortly after acceptance, before technical editing, formatting and proof reading. Using this free service, authors can make their results available to the community, in citable form, before we publish the edited article. We will replace this *Accepted Manuscript* with the edited and formatted *Advance Article* as soon as it is available.

You can find more information about *Accepted Manuscripts* in the Information for Authors.

Please note that technical editing may introduce minor changes to the text and/or graphics, which may alter content. The journal's standard Terms & Conditions and the Ethical guidelines still apply. In no event shall the Royal Society of Chemistry be held responsible for any errors or omissions in this *Accepted Manuscript* or any consequences arising from the use of any information it contains.

ROYAL SOCIETY OF CHEMISTRY

www.rsc.org/nanoscale

Please do not adjust margins

Journal Name

ARTICLE

Fluorescence Enhancement on Silver Nanoplate at the Single- and Sub-Nanoparticle Level

Received 00th January 20xx,
Accepted 00th January 20xx

DOI: 10.1039/x0xx00000x

www.rsc.org/

Yangbin Shen,[a,b] Ting He,[a,c] Wenhui Wang,[a,c] Yulu Zhan,[a,c] Xin Hu,[a,b] Binfang Yuan[a] and Xiaochun Zhou*[,a]

The fluorescence intensity of fluorescent molecule could be strongly enhanced when the molecule is near a metal nanoparticle. Hence, fluorescence enhancement has a lot of applications in the fields of biology and medical science. It is necessary to understand the mechanism for such attractive effect, if we intend to develop better materials to improve the enhancement. In this paper, we directly image the diverse patterns of fluorescence enhancement on single Ag nanoplates by super-resolution microscopy. The research reveals that the edges or tips of Ag nanoplate usually show much higher ability of fluorescence enhancement than the mid part. The spatial distribution of fluorescence enhancement strongly depends on the size of Ag nanoplate as well as the angle between Ag nanoplate and incident light. The experimental results above are essentially consistent with the simulated electric-field by the theory of localized surface plasmon resonance (LSPR), but some irregularities still exist. We also find that fluorescence enhancement on small Ag nanoplate is mainly due to in-plane dipole plasmon resonance, while the enhancement on large Ag nanoplate is mainly due to in-plane quadrupole plasmon resonance. Furthermore, in-plane quadrupole resonance of large plate has higher ability to enhance the fluorescence signal than in-plane dipole plasmon resonance. This research provides many valuable insights into the fluorescence enhancement at the single- and sub-nanoparticle level, and will be very helpful in developing better relevant materials.

1. Introduction

The fluorescence intensity of fluorescent molecule could be enhanced up to 100 times when the molecule is adjacent to metal nanoparticles.[1] Such attractive effect is very useful in detecting low concentration or single fluorescent molecules, which are widely used as labels in biology[2-6] and medical science.[7-10] Fluorescence enhancement already has some related applications, such as the detections of RNA,[11] cancer cell,[9, 12, 13] immunoassay[7] and protein.[4, 14] The enhancement can make these applications work at lower cost, faster detection rate, higher sensitivity etc. However, the fluorescence enhancement factor is far less than 100 times for most of cases.

It is necessary to understand the mechanism for such attractive effect, if people intend to develop better materials to improve the enhancement. But the mechanism of fluorescence enhancement is actually very complicated. Usually, fluorescence enhancement can be attributed to three mechanisms including local enhanced electric-field,[15] surface plasmon-coupled emission,[16] and increased radiative decay rate of fluorescent molecule.[17] In addition, some other factors, such as collection efficiency of the far-field light in the experimental geometry, also can induce fluorescence enhancement.

Hence, fluorescence enhancement is highly sensitive to many parameters, such as composition, size, shape, sharpness of nanostructure, environment surrounding the nanostructure, distance to nanoparticle, and so on. Among these parameters, the structure of nanoparticle has already been studied by many researchers due to its high significance.[18-23] For example, the spherical nanoparticle,[24] triangular nanoplate,[18, 19] nanorod,[25-27] nanowire,[20] core-shell structure[21-23] etc[28] have been proved to be effective in fluorescence enhancement. Furthermore, the fluorescence intensity could be enhanced more dramatically, when a nanoparticle was coupled with another nanostructure in a short distance.[29-31]

If the spatial distribution of fluorescence intensity is clearly resolved on a single nanostructure, we can understand the mechanism of fluorescence enhancement better. Currently, the pattern of fluorescence enhancement usually can be obtained by the simulation according to the theory of localized surface plasmon resonance (LSPR).[15, 32, 33] The simulation can predict the fluorescence enhancement, which is dependent on the local intensity of electric field. According to the simulation, we know that the electric field is unevenly distributed around

[a.] Division of Advanced Nanomaterials, Suzhou Institute of Nano-tech and Nano-bionics, Chinese Academy of Sciences, Suzhou 215125, China.
[b.] University of Chinese Academy of Sciences, Beijing 100049, China.
[c.] Shanghai University, Shanghai 200444, China.
Suzhou Institute of Nano-tech and Nano-bionics, Chinese Academy of Sciences, Suzhou 215125, China. E-mail: xczhou2013@sinano.ac.cn
†Electronic Supplementary Information (ESI) available. See DOI: 10.1039/x0xx00000x

Nanoscale Accepted Manuscript

Please do not adjust margins

Journal Name

ARTICLE

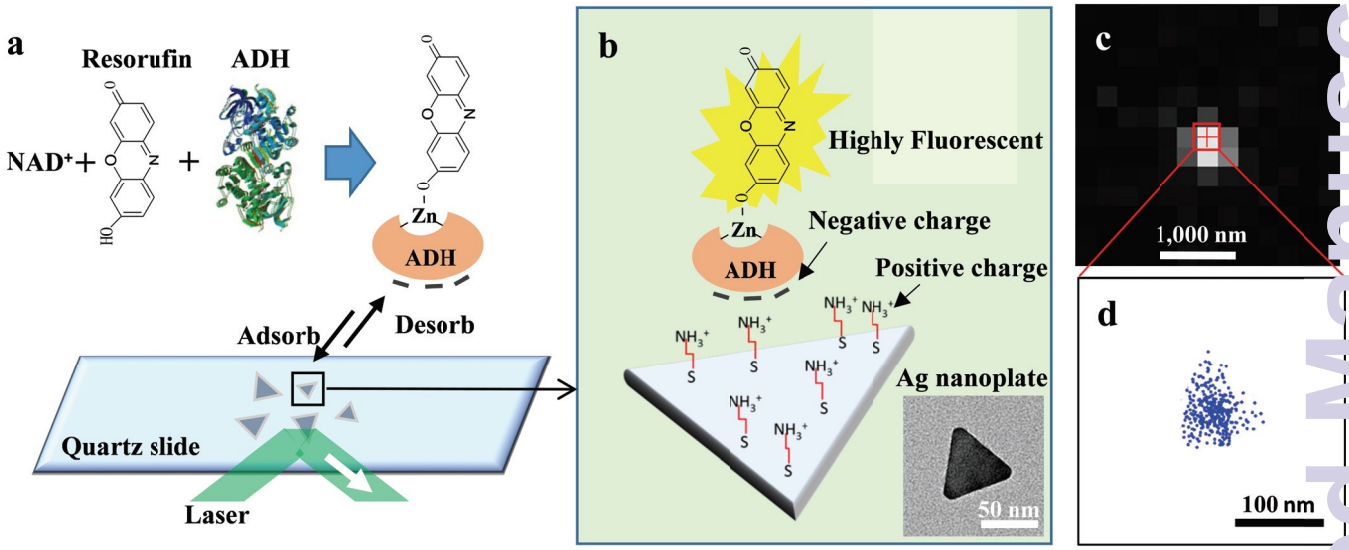

Figure 1. Localizing single resorufin molecules on a single Ag nanoplate by super-resolution microscopy. (a) Experimental design using TIRFM and microfluidic reactor to image the enzyme-substrate complex Resorufin-ADH-NAD^+ on the surface of triangular silver nanoplate. (b) Schematic of an excited enzyme-substrate complex Resorufin-ADH-NAD^+ on a single Ag nanoplate modified with 2-mercapto-ethylamine. The inset is a TEM image of a single Ag nanoplate. (c) Wide-field fluorescence image of a single resorufin molecule excited by circular polarized 532 nm laser. (d) Positions of single resorufin molecules on a single Ag nanoplate localized by super-resolution microscopy. Each dot is one resorufin molecule. There are ~366 resorufin molecules in **d**. The measurements were performed for 12 hours with 7 mM pH 6.8 phosphate buffer containing 4×10^{-4} M NAD^+, 1.125×10^4 unit/L ADH, 2.84×10^{-17} M resorufin and 32 mM L-ascorbic acid.

the nanostructure, since the LSPR is extremely sensitive to the parameters, such as size, distance and shape.[1, 29, 34, 35] Some special locations called "hot spots" have much stronger electric field than others. Consequently, the fluorescence intensity of the fluorescent molecules at these "hot spots" may be dramatically enhanced. Although the fluorescence enhancement distribution on the single nanoparticles could be simulated by theory, it is rarely uncovered by experiment directly.[35]

Actually, many researchers have done outstanding work about fluorescence enhancement and Raman enhancement on nanostructure by using super-resolution microscopy,[27, 36-38] since super-resolution microscopy is a very effective method to localize the emissive object at sub-nanoparticle accuracy.[39] Meanwhile, super-resolution microscopy also can provide some other information, such as emission intensity and polarization. Benefiting from the rapid development of the single-molecule super-resolution technology in recent years, people can image the fluorescence enhancement profile of single "hot spots" on the surfaces of aluminium thin films and silver nanoparticle clusters.[37] Super-resolution microscopy was also applied to study the surface-enhanced fluorescence on metal nanostructures.[27, 36] But the fluorescence enhancement distribution on single nanoparticle has not yet been clearly obtained. Moreover, some important and interesting parameters, such as the size of nanoparticle and the angle between nanoparticle and the incident light, have rarely been studied in fluorescence enhancement.

Here we use super-resolution microscopy to image the diverse patterns of fluorescence enhancement on single triangular silver nanoplates. The research found that the fluorescent molecules at different locations of a single Ag nanoplate have different ability of fluorescence enhancement. The pattern of fluorescence enhancement in the experiment is essentially consistent with that of simulated electro-field by finite difference time domain (FDTD) method, but is not consistent in some special cases. So our research here strongly supports the prediction in theory, and also indicates more complicated mechanism of fluorescence enhancement at the single- and sub-nanoparticle level.

2. Results and discussion

2.1. Localize the Position of Single Fluorescent Molecule on a Single Ag Nanoplate.

Nanoscale Accepted Manuscript

Triangular silver nanoplate was chosen as the fluorescence enhancement material in this paper (**Figure 1**), since silver nano-material has many advantages, such as low toxicity, low cost, high enhancement ability etc. The triangular silver nanoplates with size 30-150 nm (edge length) were synthesized by reducing silver nitrate with $NaBH_4$ according to the previous report.[40] The Ag nanoplates were immobilized on quartz slide by dropping the diluted colloidal solution on the slide directly. The Ag nanoplates were dispersed on the slide very well, and the distance between them was usually larger than 2 μm (Figure S4), which was enough to differentiate the single silver nanoplates. A microfluidic reactor was fabricated by above slide for the single nanoparticle and single molecule study as shown in **Figure 1**a and Figure S8.

The microfluidic reactor was mounted on a total internal reflection fluorescence microscope (TIRFM) to detect the fluorescence signal of single fluorescent molecule on a single Ag nanoplate. But the fluorescence might be quenched if the fluorescent molecule is too close to nanoparticle.[41] The fluorescent molecule resorufin could directly bind on the Ag nanoplate when resorufin was directly flowed into the microfluidic reactor. Consequently, the control experiment showed that very few fluorescence events were detected at this condition (Figure S5). However, previous research shows that fluorescence enhancement only happens when the fluorescent molecule has a certain distance away from the nanoparticle.[41-43] The surface of the nanoparticle was usually modified by non-metal materials, such as DNAs,[18, 29] SiO_2[44-47] and protein[48], with a controllable thickness in fluorescence enhancement research. Therefore, in this paper, alcohol dehydrogenase (ADH) (SI-2) was used as a spacer to separate the fluorescent molecule resorufin from the Ag nanoplate by several nanometers distance (**Figure 1**b).

Since ADH has an ability to interact with –OH functi group under the assistance of the coenzyme NAD^+, resorufi combined with ADH to form an enzyme-substrate comple (Resorufin-ADH-NAD^+) (**Figure 1**a). Then Resorufin-ADH-NAD^+ adsorbed onto the single Ag nanoplate by electrostat interaction (Figure S6), and was excited by a circular polarized 532 nm laser (Linear polarized laser was also tried, but cou not give enough events.) at 20 mW (**Figure 1**a-b). The single resorufin molecule gave a burst of photons, which wer detected by an EMCCD camera (**Figure 1**c). Moreover, the control experiment showed that a large number of fluorescence signals could be detected only if these three species (resorufin, ADH and NAD^+) exist at the same tim (Figure S5). This phenomenon indicates that ADH only works a the condition when all three species exist in the solution Therefore, we have successfully detected the fluorescenc signal from single resorufin molecule on single Ag nanoplate

The position of the single resorufin molecule was determined by super-resolution microscopy at the accurac ~20 nm.[49] By localizing the position of each Resorufin-ADH-NAD^+ adsorbed on the Ag nanoplate one by one, we can p the profile of the nanoplate in **Figure 1**d.[50] The profile will b clear, if there are a large number of resorufin molecules adsorbed on the nanoplate (~366 resorufin molecules in **Figur 1**d). In addition, some other valuable information, such as th size and orientation of single Ag nanoplates, could be obtained from the analysis of super-resolution microscopy. Suc information is very important for further study of fluorescence enhancement as follows.

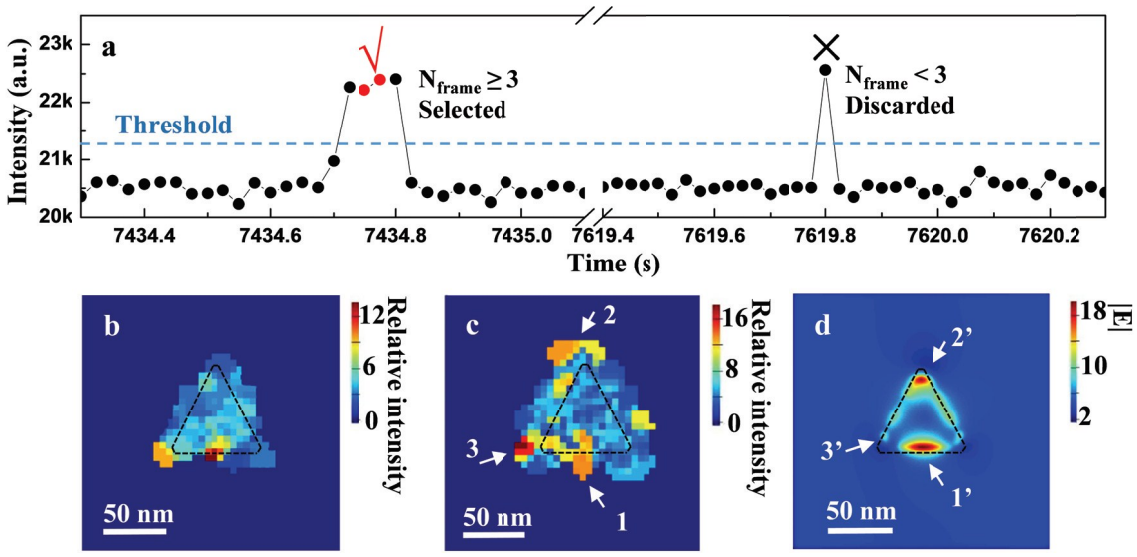

Figure 2. Fluorescence intensity at different locations on single Ag nanoplate. (a) Fluorescence intensity versus time trajectory for a single nanoplate under the adsorbing and desorbing of the enzyme-substrate complex Resorufin-ADH-NAD^+. Only th events with more than 2 on-time frames, i.e. $N_{frame} \geq 3$, will be selected out for fluorescence intensity calculation. (b) Relative intensity pattern of the fluorescence signal from single resorufin molecules on a single Ag nanoplate with the size ~70 nm (edg length). The relative intensity is calculated by dividing the intensity on each position by the lowest intensity on the Ag nanoplate. About 29 molecules are included. (c) Overlapping the relative intensity of three single Ag nanoplates with similar size. About 122 molecules are included. (d) Electric-field distribution on a single Ag nanoplate with the size 70 nm simulated by FDTD method.

Nanoscale Accepted Manuscript

Journal Name

ARTICLE

Nanoscale Accepted Manuscript

2.2. Spatial Distribution of Fluorescence Intensity on a Single Ag Nanoplate

Although **Figure 1**d presents the positions of resorufin molecules, it can't give the accurate fluorescence intensity of them. Since the fluorescence intensity is the number of photons within a unit time, its calculation needs to obtain both the number of photons and the corresponding duration time of emission. However, fluorescent molecule usually is not always emissive in the first frame and last frame of on-time (**Figure 2**a). Therefore, the first frame and last frame of on-time can't be taken into account in fluorescence intensity calculation. That is to say only the frames in the mid part of on-time can be used to calculate the fluorescence intensity.

In order to calculate the fluorescence intensity of the single resorufin molecules, only the events with more than 2 on-time frames, i.e. $N_{frame} \geq 3$, will be selected out for further analysis (**Figure 2**a). Then, the mid frames of on-time (red dots in **Figure 2**a) are combined together to one frame, which is fitted by a two dimensional Gaussian function to calculate the fluorescence intensity of single resorufin molecule. The intensity of each molecule will be divided by the number of mid frames in on-time. At last, the positions of the single resorufin molecules are plotted with their intensity in **Figure 2**b. The spatial range of the intensity will be extended to a round, whose center and radius are the position and the error bar of position from Gaussian fitting as shown in **Figure 2**b, respectively. If there is overlapping between neighbour molecules, the maximum intensity will be used.

Figure 2b shows that the fluorescence intensity is not evenly distributed on a single Ag nanoplate with the size ~70 nm (edge length). Some "hot spots", which are near the edges and tips, have much higher fluorescence intensity than others, indicating stronger local fluorescence enhancement effect. For example, **Figure 2**b shows that the bottom of the nanoplate has the strongest fluorescence intensity, which is ~12 times higher than the weakest location. By overlapping the relative intensity of three single Ag nanoplates, more "hot spots" are localized in **Figure 2**c. So we achieve the challenging work of directly imaging the "hot spots" for the fluorescence enhancement on a single nanoparticle at sub-nanoparticle accuracy.

Figure 2d shows that the simulated pattern of electric-field intensity essentially agrees with the pattern of fluorescence intensity in **Figure 2**b and c. For example, fluorescent molecules at the positions 1' and 2' in **Figure 2**d have higher fluorescence intensity, which is similar as those at the positions 1 and 2 in **Figure 2**c. So the fluorescence enhancement on single Ag nanoplate is mainly due to the enhanced electric field by LSPR.

However, the simulation in theory cannot predict all the positions with higher fluorescence intensity. For an example, electric-field intensity at the positions 3' in **Figure 2**d is not very high, while fluorescent molecules at the positions 3 in **Figure 2**c have the highest fluorescence intensity. This phenomenon is actually observed in many other single Ag nanoplates (Figure S11). So there should be other factors, such as the orientation of molecule, more structure details environment surrounding the nanostructure etc, affecting the local fluorescence intensity at the single nanoparticle level. Further work needs to be done to reveal the mechanism of such kind of fluorescence enhancement. Therefore, this work not only strongly supports the prediction from the simulation but also reveals that there are other factors strongly affect the fluorescence enhancement, simultaneously.

2.3. Size and Spectrum Dependent Fluorescence Enhancement on Single Ag Nanoplate.

In order to study the size dependent fluorescence enhancement, it's necessary to obtain the size of each single Ag nanoplate first. Unfortunately, it is very difficult to directly measure the size of a single Ag nanoplate on glass slide in microfluidic reactor. In this paper, the size of Ag nanoplate was measured by the profile of single nanoplate in super-resolution imaging. On the other hand, people are also interested in spectrum dependent fluorescence enhancement. In order to measure the LSPR spectra of many single Ag nanoplates more efficiently, we developed a homebuilt spectrometer to massively screen the spectra of many single Ag nanoplates during one time of measurement (SI-6). Actually, size and spectrum dependent fluorescence enhancement have very close relationship, since the LSPR spectrum of Ag nanoplate has strong correlation with its size (SI-8).[51, 52]

In common research, the fluorescence enhancement can be expressed as,

$$r = \frac{I}{I_{free}} \quad (1)$$

Where r is fluorescence enhancement factor, I is the fluorescence intensity of single molecule in research, and I_{free} is the fluorescence intensity of free molecule at the same condition. However, we cannot obtain the I_{free} in this research, because no free molecule was detected in our experiment (the detected molecules were all on the Ag nanoplates). In order to compare the fluorescence enhancement ability between different nanoparticles, the normalized fluorescence intensity (NFI) by the local intensity of excitation light is calculated,

$$r' = \frac{I}{I_{local}} \quad (2)$$

Please do not adjust margins

Journal Name

ARTICLE

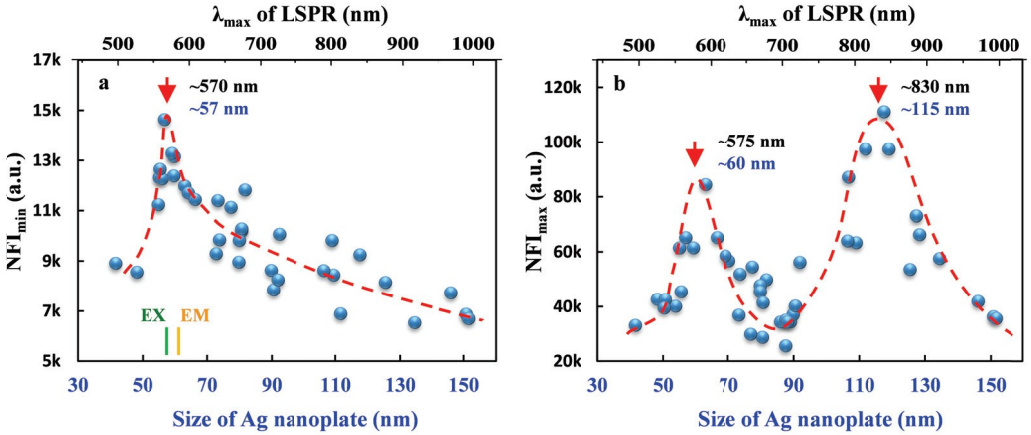

Figure 3. Minimum NFI (a) and maximum NFI (b) of single Ag nanoplates with different sizes or λ_{peak}. The arrows point the peak locations of NFI. The black word near the arrow is the λ_{max} of LSPR, while the blue word is the size of Ag nanoplate. The green (EX) and yellow (EM) lines in **a** mark the position of the maximum excitation wavelength of resorufin (~571 nm) and the maximum emission wavelength of resorufin (~585 nm).

Where *r'* is the NFI, I_{local} is the local intensity of excitation light. Since the fluorescence intensity is dependent on the intensity of excitation light,

$$I_{free} = kI_{local} \quad (3)$$

Then,

$$r' = kr \quad (4)$$

So the *r'* is proportional to fluorescence enhancement factor, and can be used to compare the fluorescence enhancement ability between different molecules on different nanoparticles. In the experiment, the fluorescence intensity of each fluorescent molecule can be normalized by the intensity of excitation light. The *r'* has an advantage that it is independent on the local intensity of excitation light. So we can compare the *r'* for the single Ag nanoplates at different locations with different local intensities of excitation light.

Figure 3a shows the lowest NFI, i.e. NFI_{min}, on single Ag nanoplates versus the size of Ag nanoplate. There is a peak appears at λ_{max} = ~570 nm (or ~57 nm size of Ag nanoplate), which is very close to the maximum excitation wavelength of resorufin (~571 nm). In this paper, this means that the brightest fluorescence will be observed if the dye is absorbed to particles with LSPR peaks at ~570 nm.[18] This wavelength is slightly lower than the maximum emission wavelength of resorufin (~585 nm), but quite higher than the wavelength of the excitation light in the experiment (532 nm). Therefore, fluorescence intensity of a dye absorbed to a silver nanoparticle is also strongly dependent on the overlap between the LSPR of the nanoparticle with the spectral properties of the dye. The literatures suggest that the most fluorescence intensity is observed when the dye emission peak is redshifted from the LSPR peak.[18, 53] Our research here strongly verifies the rule they found.[18] Moreover, our research covers a larger range of LSPR wavelength from ~500 to ~1000 nm comparing to literature.[18] We further see that NFI_{min} on single Ag nanoplates keeps decreasing after 700 nm. Therefore, the rule in literature is still working for NFI_{min} after 700 nm.

By looking into the pattern of fluorescence intensity in **Figure 2** (SI-6 and SI-7), we can more deeply understand the relationship between NFI_{min} versus the size. These figures show that the minimum intensity usually exists at the center of the nanoplate for all size. For smaller size, the whole nanoplate is excited, and the minimum intensity |E| at the center is usually bigger than 10. But, for the bigger size, only the tips and edges are excited, and the minimum intensity |E| at the center is usually less than 2. This might be the reason for the decay of the minimum intensity with the increase of size.

Interestingly, **Figure 3b** shows that the highest normalized fluorescence intensity NFI_{max} on single Ag nanoplates has two peaks with the increase of size. The first peak appears at λ_{max} = ~575 nm (or ~60 nm size of Ag nanoplate), which is almost same as that in **Figure 3a.** The enhancement mechanism of the highest fluorescence should be similar as that of the lowest one in the wavelength range from ~500 to ~700 nm. That is to say either the mid part or edges and corners of a single Ag nanoplate have the similar enhancement mechanism at such wavelength range.

Nanoscale Accepted Manuscript

Please do not adjust margins

However, besides the peak at λ_{max} = ~575 nm, there is a second peak appears at λ_{max} = ~830 nm (or ~115 nm size of Ag nanoplate) for NFI_{max}. This peak is not observed in **Figure 3a** nor by other researchers.[15] This wavelength is far from the wavelength of excitation light and the fluorescence of resorufin. What's the reason for the appearance of this peak?

In order to find the reason for the appearance of the second peak, the full spectra of large Ag nanoplates are shown in Figure 4**a**. There is indeed another strong LSPR peak from 500 to 600 nm for such big nanoplate. As we all know that the silver nanoplate exhibit three absorption peaks with different intensity, assigned to the in-plane dipole plasmon resonance, in-plane quadrupole resonance and out-plane quadrupole resonance, respectively.[54-56] The LSPR peak from 500 to 600 nm for such big nanoplate could be assigned to in-plane

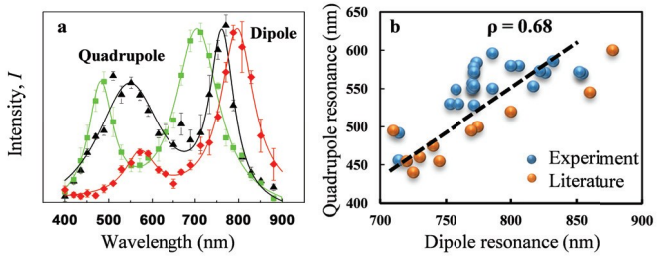

Figure 4. (a) Spectrum of single Ag nanoplates with different sizes, i.e. ~88 nm (round), ~99 nm (triangular), ~108 nm (diamond). (b) Relationship between the peak wavelength of dipole plasmon resonance and quadrupole plasmon resonance. The blue and yellow dots are from experiment and literature,[40, 54, 57-59] respectively. The Pearson's correlation coefficient is 0.68.

quadrupole resonance. Figure 4**a** shows that the peaks of both the in-plane dipole plasmon resonance and in-plane quadrupole resonance increase with the size of the Ag nanoplate.[54, 57, 60] The Pearson's correlation coefficient between these two types of plasmon resonance is up to 0.68 as shown in Figure 4**b**.

Especially, the larger Ag nanoplate (~115 nm) has a ~830 nm absorption peak of in-plane dipole plasmon resonance, and corresponding absorption peak of in-plane quadrupole resonance is ~570 nm.[61, 62] This peak wavelength (~570 nm) is as same as that of in-plane dipole resonance for smaller Ag nanoplate ~60 nm in **Figure 3**. For the larger Ag nanoplate (~115 nm), the highest normalized fluorescence intensity NFI_{max} on single Ag nanoplates has a peak in **Figure 3b**. Therefore, the rule that fluorescence intensity of a dye absorbed to a silver nanoparticle is strongly dependent on the overlap between the LSPR of the nanoparticle with the spectral properties of the dye is still working. The second peak of fluorescence enhancement in **Figure 3b** could be attributed to in-plane quadrupole resonance.

In fact, the absorption peak of in-plane quadrupole resonance is a relatively weaker than that of in-plane dipole resonance in Figure 4**a**. Such weak peak of in-plane quadrupole resonance rarely attracts much attention for the fluorescence enhancement research, although quadrupole resonance also can contribute to the near-field enhancement of nanoparticle.[57, 60] Our research indicates that the weaker absorption peak of in-plane quadrupole resonance could have higher ability to enhance the fluorescence. If we look into the simulated electric-field intensity pattern in Figure S10, we can find that the tiny area on the sharp corner or edge still have a strong electric-field on large nanoplate. The maximum intensity |E| at the corner or edge for big size nanoplate is usually up to 20, which is stronger than that for small size nanoplate. So in-plane quadrupole resonance has very high ability to enhance the local intensity of electric-field on nanoplate, and enhance the fluorescence intensity.

Moreover, the intensity of the second peak for larger size is higher than that of the first peak at smaller size in **Figure 3b**. In addition, quadrupole resonance is much easier to happen on larger size of nanoparticle, which is usually stabler and easier to synthesize than smaller size one. Therefore, the quadrupole resonance mode might provide an effective way to induce higher signal of SERS and surface-enhanced fluorescence.[63, 64] This finding is helpful to develop high-quality nano-materials with higher fluorescence enhancement.

2.4. Size and Spectrum Dependent Inhomogeneity of Fluorescence Enhancement on a Single Ag Nanoplate.

To compare the inhomogeneity of fluorescence enhancement at different positions within a single nanoparticle, an intraparticle fluorescence enhancement factor (IPFEF) is defined in this paper. The IPFEF for experiment is defined as dividing the highest 10% fluorescence intensities by the lowest 10% ones on the same single Ag nanoplate, while the IPFEF for simulation is defined as dividing the highest 10% electric-field intensities by the lowest 10% ones on the same single Ag nanoplate. So IPFEF can be expressed as,

$$IPFEF = \frac{\text{highest 10\% fluorescence/electric-field intensities}}{\text{lowest 10\% fluorescence/electric-field intensities}} \quad (5)$$

The IPFEF has an advantage that it is independent on the intensity of light field. Although the light field of excitation light is inhomogeneous in the field of vision (~100 μm × 50 μm), the intensity of excitation light on one nanoplate is almost homogeneous since single nanoplate is small enough (less than 200 nm). So the IPFEF can reflect the fluorescence enhancement effect within the same single nanoplate.

Figure 5a shows the variation of IPFEF versus the size or λ_{peak} of single Ag nanoplates. With the increase of size or λ_{peak}, IPFEF increases for both experiment and simulation. The higher IPFEF means larger spatial inhomogeneity of fluorescence intensity on the same nanoplate. Obviously, the IPFEF in theory is up to ~30, which is much higher than ~12 in experiment. One possible reason for the difference is that the simulation result has much higher spatial resolution (~2 nm), which can find the locations with higher IPFEF. But the spatial resolution of super-resolution microscopy is ~20 nm, which is possible to miss some locations with higher IPFEF. Another possible reason is that the energy transfer from electric field to fluorescent molecule is not efficient enough.

Nanoscale Accepted Manuscript

This journal is © The Royal Society of Chemistry 20xx

Please do not adjust margins

Journal Name

ARTICLE

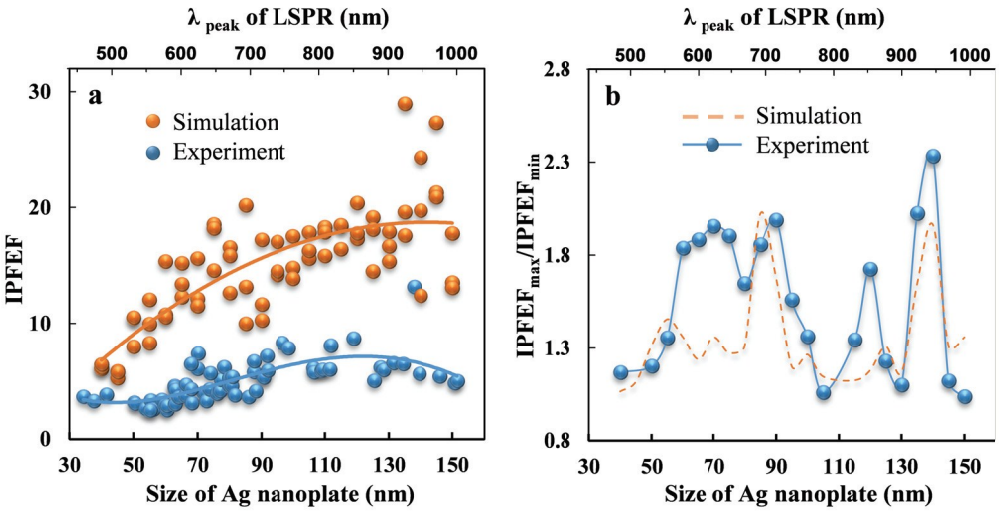

Figure 5. Size dependent fluorescence enhancement on single Ag nanoplate. (a) Variation of intraparticle fluorescence enhancement factor (IPFEF) versus the size or λ_{peak} of single Ag nanoplates. Simulation at each size is performed at three angles, i.e. 0°, 15°, 30°, between Ag nanoplate and incident light. The curves are for visual guidance. (b) The ratio $IPFEF_{max}/IPFEF_{min}$ in a versus the size or λ_{peak} of single Ag nanoplates.

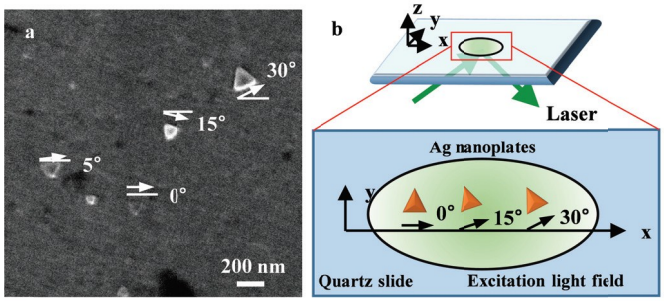

Figure 6. SEM image and schematic of the singe Ag nanoplates with different orientations. (a) SEM image of the singe Ag nanoplates with different orientations on ITO slide. The Ag nanoplates are proved to lie down on the slide. Higher concentration of Ag nanoplates was used to increase the density of Ag nanoplate. (b) Schematic of three examples, which have different angles, i.e. 0°, 15°, 30°, between nanoplate and incident light.

2.5. Angle Dependent Fluorescence Enhancement on a Single Ag Nanoplate.

It is worth noting that the results for both experiment and simulation scatter around the visual guidance curves in **Figure 5**a. For an example, the IPFEFs vary a lot even at the similar size ~90 nm. We plot the ratio between the maximum IPFEF and minimum IPFEF ($IPFEF_{max}/IPFEF_{min}$) in a certain range of size as shown in **Figure 5**b. The ratio from experiment (blue dots) agrees well with that from the simulation (yellow dash curve). Moreover, **Figure 5**a shows that the variation of IPFEF for simulation is due to the angle between Ag nanoplate and incident light. Therefore, the IPFEF for experiment is at least partly angle dependent. Besides the simulation, we indeed see that the orientations of Ag nanoplates are different from particle to particle in experiment. **Figure 6**a shows that the orientations of Ag nanoplates are randomly distributed, since the Ag nanoplates are immobilized by directly dropping the colloidal solution of Ag nanoplate onto quartz slide. **Figure 6**b shows the schematic of the singe Ag nanoplates with different angles between nanoplate and the incident light. But we couldn't take any clear image for the nanoplates on quartz slide due to the non-conductivity of quartz slide and the thin thickness of nanoplate (~7 nm), even if the quartz slide is coated with a layer of carbon or gold.

In order to see the effect of angle in detail, **Figure 7** presents some representative nanoplates with same size ~55 nm at different angles, i.e. 0°, 15°, 30°. The patterns of fluorescence intensity on single Ag nanoplates vary a lot with the change of angle. These different patterns indicate the fluorescence enhancement strongly depends on the orientation of single Ag nanoplate. For an example, **Figure 7**a-c show that the location of the highest intensity varies with the increase of angle. **Figure 7**d shows that the maximum enhancement decreases with the increase of angle (more examples in Figure S11).

Nanoscale Accepted Manuscript

Please do not adjust margins

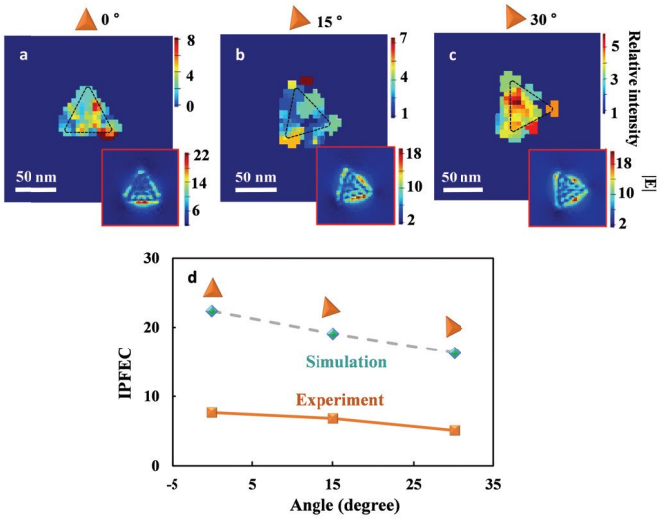

Figure 7. Distributions of fluorescence intensity and simulated electric-field intensity for the single Ag nanoplates with different angles between nanoplate and incident light. (a-c) Distributions of fluorescence intensity (big panel) and simulated electric-field intensity (small panel with red frame) for the single Ag nanoplates with the same size ~55 nm at different angles (i.e. 0°, 15°, 30°). (d) IPFEF for the Ag nanoplates in **a**, **b**, **c**. The orange squares and curve are the IPFEF in experiment, while the green diamonds and curve are the IPFEF in theory.

3. Conclusions

In this paper, super-resolution microscopy is applied to directly image the pattern of fluorescence enhancement on single Ag nanoplate. The research reveals that the fluorescence intensity of single fluorescent molecule is unevenly distributed on a single Ag nanoplate. In most cases, the fluorescent molecule on the edges or tips of Ag nanoplate has higher fluorescence intensity, while the molecule in the mid part has lower intensity. So the edges or tips of Ag nanoplate usually show relatively higher ability of fluorescence enhancement. The patterns of fluorescence enhancement also vary with the size of Ag nanoplate and the angle between Ag nanoplate and incident light. It is found that fluorescence enhancement on small Ag nanoplate is mainly due to in-plane dipole plasmon resonance, while the enhancement on large Ag nanoplate is mainly due to in-plane quadrupole resonance. Furthermore, the in-plane quadrupole resonance of large nanoplate has higher ability to enhance the fluorescence signal than in-plane dipole plasmon resonance. Most of above experimental results can be interpreted by the electric-field simulation, but some special ones still can't be. Especially, the simulation cannot predict some certain locations with much higher ability of fluorescence enhancement on single Ag nanoplate. In future research, it is still necessary to use super-resolution microscopy to reveal the mechanism of fluorescence enhancement on single nanoparticle, and design better materials.

4. Experimental

4.1. Preparation of triangular silver nanoplate.

We synthesized the triangular silver nanoplates with size 30-150 nm (edge length) by reducing silver nitrate with $NaBH_4$ and H_2O_2 according to the previous report.[40] The UV-vis spectrum of the Ag nanoplate has a broad peak at ~600 nm (SI-3), which means the size of nanoplate is not uniform. The average size of the nanoplate is ~60 nm measured by TEM (Figure S3).

4.2. Single molecule and single nanoparticle experiment.

A microfluidic reactor was fabricated according our previous work[50] (refer SI-6 for more details). The surface plasmon resonance spectrum of single nanoplates was measured by a homebuilt spectrometer (SI-6). In order to image the fluorescent molecule on Ag nanoplates, a super-resolution imaging was performed by an Olympus IX71 microscope. The single Ag nanoplates were excited by a 532 nm laser in TIRFM. The excitation spot size is ~100 μm × 50 μm. The fluorescence signal was collected by a 60X NA1.2 water immersion objective, and detected by an ANDOR Ixon DU 897D-CS0-#BV EMCCD camera operated at 25 ms frame rate. More than 1.5 million frames were recorded in order to detect enough number of single fluorescence molecules. The gold nanoparticles with an average diameter of ~45 nm were prepared and used as markers for the drift correction in super-resolution imaging.[50, 65]

To increase the number of events, we let ADH and Ag nanoplate carry different types of charges (**Figure 1**b). In order to let Ag nanoplate carry some positive charges, the nanoplate was modified by 2-mercapto-ethylamine (**Figure 1b**). The –SH group of the 2-mercapto-ethylamine can bind on the nanoplate through S-Ag bond firmly, while the $–NH_2$ group will expose to the solution. Ag nanoplate will carry some positive charges if pH value is lower than 10.6. On the other hand, in order to let ADH carry some negative charges, pH value should be higher than the isoelectric point of ADH 5.4~5.8. Moreover, these negative charges will be concentrated at some areas with more carboxyl groups to form some negative charge areas (SI-2). These areas have higher affinity to bind on the positively charged surface of single Ag nanoplate, and facilitate the adsorption of the enzyme-substrate complex Resorufin-ADH-NAD^+. By trying several pH values, we found that the optimum pH value is 6.8, where the largest number of events was obtained (SI-5).

4.3. Binding of ADHs on single Ag nanoplates.

In the first step, the Ag nanoplates were modified with 5 mM 2-mercapto-ethylamine for 10 min at a flow rate 8 μL/min to make the Ag nanoplates take positive charges. In the second step, the residue 2-mercapto-ethylamine was washed off by pH 6.8 phosphate buffer for 10 min at the same flow rate. In the third step, 1.125×10^4 unit/L ADHs in pH 6.8 phosphate buffer was injected into the flow cell for 20 min at 8 μL/min. In the fourth step, phosphate buffer containing 4×10^{-4} M NAD$^+$,

Nanoscale Accepted Manuscript

This journal is © The Royal Society of Chemistry 20xx

1.125×10^{4} unit/L ADH, 2.84×10^{-17} M resorufin and 32 mM L-ascorbic acid, was injected into the microfluidic reactor at the flow rate 8 μL/min. L-ascorbic acid was used as a reducing substances to protect the Ag nanoplates from the corrosion of light and oxygen. Since the ADH carries negative charges and Ag nanoplate carries positive charges, the binding of ADH will happen on Ag nanoplates.

4.4. Simulation of electric-field distribution on the nanoplate.

The electric-field distribution on the nanoplate was simulated by FDTD method, which was widely used for the electric-field simulation of nanoparticle. The evanescent wave with circular polarization was simulated by 532 nm wavelength laser. During the simulation, many parameters, such as the refractive index of solution and quartz slide, direction of incident light, angle between nanoplates and incident light and so on, were taken into account. The spatial precision is 2 nm.

Acknowledgements

This work was supported by the National Natural Science Foundation of China (No. 21373264, No. 21573275), Suzhou Institute of Nano-tech and Nano-bionics (Y3AAA11004) and Thousand Youth Talents Plan (Y3BQA11001).

References

1. G. P. Acuna, F. M. Moeller, P. Holzmeister, S. Beater, B. Lalkens and P. Tinnefeld, *Science*, 2012, **338**, 506-510.
2. H. Jans and Q. Huo, *Chem. Soc. Rev.*, 2012, **41**, 2849-2866.
3. K. Saha, S. S. Agasti, C. Kim, X. Li and V. M. Rotello, *Chem. Rev.*, 2012, **112**, 2739-2779.
4. H. Li, M. Wang, W. Qiang, H. Hu, W. Li and D. Xu, *Analyst*, 2014, **139**, 1653-1660.
5. H. Li, C.-Y. Chen, X. Wei, W. Qiang, Z. Li, Q. Cheng and D. Xu, *Anal. Chem.*, 2012, **84**, 8656-8662.
6. P. D. Howes, R. Chandrawati and M. M. Stevens, *Science*, 2014, **346**, 1247390.
7. L. Zhou, F. Ding, H. Chen, W. Ding, W. Zhang and S. Y. Chou, *Anal. Chem.*, 2012, **84**, 4489-4495.
8. B. Zhang, R. B. Kumar, H. Dai and B. J. Feldman, *Nat. Med.*, 2014, **20**, 948-953.
9. H. Cho, E.-C. Yeh, R. Sinha, T. A. Laurence, J. P. Bearinger and L. P. Lee, *ACS nano*, 2012, **6**, 7607-7614.
10. D. A. Giljohann and C. A. Mirkin, *Nature*, 2009, **462**, 461-464.
11. K. Aslan, J. Huang, G. M. Wilson and C. D. Geddes, *J. Am. Chem. Soc.*, 2006, **128**, 4206-4207.
12. W. Hu, Y. Liu, H. Yang, X. Zhou and C. M. Li, *Biosens. Bioelectron.*, 2011, **26**, 3683-3687.
13. K. A. Homan, M. Souza, R. Truby, G. P. Luke, C. Green, E. Vreeland and S. Emelianov, *Acs Nano*, 2012, **6**, 641-650.
14. H. Mishra, A. Dragan and C. D. Geddes, *J. Phys. Chem. C*, 2011, **115**, 17227-17236.
15. Y. Zhang, A. Dragan and C. D. Geddes, *J. Phys. Chem. C*, 2009, **113**, 15811-15816.
16. J. R. Lakowicz, *Anal. Biochem.*, 2001, **298**, 1-24.
17. H. Nabika and S. Deki, *J. Phys. Chem. B*, 2003, **107**, 9161-9164.
18. Y. Chen, K. Munechika and D. S. Ginger, *Nano Lett.*, 2007, **7**, 690-696.
19. K. Aslan, J. R. Lakowicz and C. D. Geddes, *J. Phys. Chem. A*, 2005, **109**, 6247-6251.
20. B. Abel, S. Coskun, M. Mohammed, R. Williams, H. E. Unalan and K. Aslan, *J. Phys. Chem. C*, 2014, **119**, 675-684.
21. J. Yang, F. Zhang, Y. Chen, S. Qian, P. Hu, W. Li, Y. Deng, Y. Fang, L. Han and M. Luqman, *Chem. Commun.*, 2011, **47**, 11618-11620.
22. P. Reineck, D. Gómez, S. H. Ng, M. Karg, T. Bell, P. Mulvaney and U. Bach, *ACS nano*, 2013, **7**, 6636-6648.
23. R. Bardhan, N. K. Grady, J. R. Cole, A. Joshi and N. J. Halas, *ACS Nano*, 2009, **3**, 744-752.
24. R. Gill, L. Tian, W. R. Somerville, E. C. Le Ru, H. van Amerongen and V. Subramaniam, *J. Phys. Chem. C*, 2012, **116**, 16687-16693.
25. H. Yuan, S. Khatua, P. Zijlstra, M. Yorulmaz and M. Orrit, *Angew. Chem. Int. Ed.*, 2013, **52**, 1217-1221.
26. S. Khatua, P. M. Paulo, H. Yuan, A. Gupta, P. Zijlstra and M. Orrit, *ACS nano*, 2014, **8**, 4440-4449.
27. K. L. Blythe, E. J. Titus and K. A. Willets, *ChemPhysChem*, 2014, **15**, 784-793.
28. C. Ayala-Orozco, J. G. Liu, M. W. Knight, Y. Wang, J. K. Day, P. Nordlander and N. J. Halas, *Nano Lett.*, 2014, **14**, 2926-2933.
29. J. Zhang, Y. Fu, M. H. Chowdhury and J. R. Lakowicz, *Nano Lett.*, 2007, **7**, 2101-2107.
30. D. Marinica, A. Kazansky, P. Nordlander, J. Aizpurua and A. G. Borisov, *Nano Lett.*, 2012, **12**, 1333-1339.
31. C. Ciracì, R. Hill, J. Mock, Y. Urzhumov, A. Fernández-Domínguez, S. Maier, J. Pendry, A. Chilkoti and D. Smith, *Science*, 2012, **337**, 1072-1074.
32. G. Zoriniants and W. L. Barnes, *New Journal of Physics*, 2008, **10**.
33. M. Oszajca, C. Lincheneau, M. Amelia, C. Schäfer, K. Szaciłowski and A. Credi, *Eur. J. Inorg. Chem.*, 2013, **2013**, 3556.
34. A. Bek, R. Jansen, M. Ringler, S. Mayilo, T. A. Klar and J. Feldmann, *Nano Lett.*, 2008, **8**, 485-490.
35. B. Fu, J. D. Flynn, B. P. Isaacoff, D. J. Rowland and J. S. Biteen, *J. Phys. Chem. C*, 2015, **119**, 19350-19358.
36. H. Lin, S. P. Centeno, L. Su, B. Kenens, S. Rocha, M. Sliwa, J. Hofkens and H. Uji-i, *ChemPhysChem*, 2012, **13**, 973-981.
37. H. Cang, A. Labno, C. Lu, X. Yin, M. Liu, C. Gladden, Y. Liu and X. Zhang, *Nature*, 2011, **469**, 385-388.
38. K. A. Willets, S. M. Stranahan and M. L. Weber, *J. Phys. Chem. Lett.*, 2012, **3**, 1286-1294.
39. W. Wang, J. Gu, T. He, Y. Shen, S. Xi, L. Tian, F. Li, H. Li, L. Yan and X. Zhou, *Nano Research*, 2015, **8**, 441-455.
40. Q. Zhang, N. Li, J. Goebl, Z. Lu and Y. Yin, *J. Am. Chem. Soc.*, 2011, **133**, 18931-18939.
41. P. Anger, P. Bharadwaj and L. Novotny, *Phys. Rev. Lett.*, 2006, **96**, 113002.
42. E. Dulkeith, M. Ringler, T. Klar, J. Feldmann, A. Munoz Javier and W. Parak, *Nano Lett.*, 2005, **5**, 585-589.
43. D. Cheng and Q.-H. Xu, *Chem. Commun.*, 2007, 248-250.

Nanoscale Accepted Manuscript

44. K. Aslan, M. Wu, J. R. Lakowicz and C. D. Geddes, *J. Am. Chem. Soc.*, 2007, **129**, 1524-1525.
45. D. Cheng and Q. H. Xu, *Chem. Commun.*, 2007, DOI: 10.1039/b612401a, 248-250.
46. S. Damm, S. Fedele, A. Murphy, K. Holsgrove, M. Arredondo, R. Pollard, J. N. Barry, D. P. Dowling and J. H. Rice, *Appl. Phys. Lett.*, 2015, **106**, 183109.
47. J. Yang, F. Zhang, Y. Chen, S. Qian, P. Hu, W. Li, Y. Deng, Y. Fang, L. Han, M. Luqman and D. Zhao, *Chem. Commun.*, 2011, **47**, 11618-11620.
48. C. D. Geddes, H. Cao, I. Gryczynski, Z. Gryczynski, J. Y. Fang and J. R. Lakowicz, *J. Phys. Chem. A*, 2003, **107**, 3443-3449.
49.M. Bates, B. Huang, G. T. Dempsey and X. W. Zhuang, *Science*, 2007, **317**, 1749-1753.
50. X. Zhou, N. M. Andoy, G. Liu, E. Choudhary, K.-S. Han, H. Shen and P. Chen, *Nat. Nanotechnol.*, 2012, **7**, 237-241.
51. R. C. Jin, Y. C. Cao, E. C. Hao, G. S. Metraux, G. C. Schatz and C. A. Mirkin, *Nature*, 2003, **425**, 487-490.
52. J. Zeng, S. Roberts and Y. Xia, *Chem.-Eur. J.*, 2010, **16**, 12559-12563.
53. F. Tam, G. P. Goodrich, B. R. Johnson and N. J. Halas, *Nano Lett.*, 2007, **7**, 496-501.
54. Y. Yang, S. Matsubara, L. Xiong, T. Hayakawa and M. Nogami, *J. Phys. Chem. C*, 2007, **111**, 9095-9104.
55. Q. Zhang, J. Ge, T. Pham, J. Goebl, Y. Hu, Z. Lu and Y. Yin, *Angew. Chem. Int. Ed.*, 2009, **48**, 3516-3519.
56. R. C. Jin, Y. W. Cao, C. A. Mirkin, K. L. Kelly, G. C. Schatz and J. G. Zheng, *Science*, 2001, **294**, 1901-1903.
57.X. Zou and S. Dong, *J. Phys. Chem. B*, 2006, **110**, 21545-21550.
58. L. J. Sherry, R. Jin, C. A. Mirkin, G. C. Schatz and R. P. Van Duyne, *Nano Lett.*, 2006, **6**, 2060-2065.
59. D. Charles, M. Gara, D. Aherne, D. Ledwith, J. Kelly, W. Blau and M. Brennan-Fournet, *Plasmonics*, 2011, **6**, 351-362.
60. M. Shopa, K. Kolwas, A. Derkachova and G. Derkachov, *Opto-Electron. Rev.*, 2010, **18**, 421-428.
61. J. E. Millstone, S. Park, K. L. Shuford, L. Qin, G. C. Schatz and C. A. Mirkin, *J. Am. Chem. Soc.*, 2005, **127**, 5312-5313.
62. T. K. Sau, A. L. Rogach, F. Jaeckel, T. A. Klar and J. Feldmann, *Adv. Mater.*, 2010, **22**, 1805-1825.
63. M. J. Mulvihill, X. Y. Ling, J. Henzie and P. Yang, *J. Am. Chem. Soc.*, 2010, **132**, 268-274.
64. A. Kinkhabwala, Z. Yu, S. Fan, Y. Avlasevich, K. Mullen and W. E. Moerner, *Nat Photon*, 2009, **3**, 654-657.
65. G. Frens, *Nature*, 1972, 20-22.

Nanoscale Accepted Manuscript

This journal is © The Royal Society of Chemistry 20xx